

Nanometric measurement of optical pressure deformation of fluid interface by digital holography

David C. Clark* and Myung K. Kim

Digital Holography and Microscopy Laboratory, Physics Department, University of South Florida, 4202 E. Fowler Avenue, Tampa, Florida 33620, USA

ABSTRACT

Digital Holographic Microscopy produces quantitative phase analysis of a specimen with excellent optical precision. In the current study, this imaging method has been used to measure induced thermal lensing by optical excitation in the time-resolved regime with excellent agreement to model predictions. We have found that the thermal effect should not be dismissed when pursuing optical radiation pressure experiments, even when the media involved are transparent. We have developed a unified model and simulated methods of decoupling the two effects. The results of this study and simulations suggest that our near term goal of nanometric measurement of an optical pressure induced deformation will prove successful. Precise measurement of this phenomenon can be useful in determining physical properties of interfacial surfaces, such as surface tension, and characterizing physical properties of cellular structures.

Keywords: Digital holography, holography, optical pressure, thermal lens, cellular analysis

1. INTRODUCTION

Optical radiation pressure effects can be a very useful tool in soft matter physics for the efficient characterization of fluid interfaces and membranes. Although it is one of the most noninvasive methods, very little work has been done in this area due to the difficulty in observing these effects. Surface deformation on a fluid interface by optical radiation pressure using a continuous wave laser source is typically very weak. The output power of these lasers, even when focused tightly on the surface, is often insufficient to overcome the surface tensions of most fluid interfaces enough to form readily observable deformations. For this reason, pulse laser sources are often used to amplify laser intensity and, therefore, the resulting deformation to a more easily observable level¹. Alternatively, standard liquids have been replaced with well engineered temperature sensitive phase-separating microemulsions which will form a fluid-fluid interface with exceptionally reduced surface tension near a critical temperature^{2,3}. The method often used to sense these deformations is far-field diffraction. The bent surface of a fluid acts as a lens and the profile of the exiting laser beam¹⁻³, or separate probing laser beam⁴, can be scanned to deduce the shape and size of the deformation.

It was our intent to use the method of digital holographic microscopy to image such deformations with nanometric precision and length scales. The quantitative phase analysis inherent to digital holography^{5,6} yields an imaging method which can observe very slight surface deformations of standard fluid-fluid interfaces by true continuous wave optical radiation effects. The stable nature of the cw laser is preferred to a pulse laser for improved static surface property determination. The freedom to choose from a potentially broad selection of fluids is advantageous as the optical properties are likely to be well known making conversion of the optical phase images to real physical deformations quite straightforward. The relationship between surface deformation by known optical forces and other important surface properties, such as surface tension and viscosity, has previously been derived^{7,8}.

We have found that many studies on optical radiation pressure dismiss thermal effects simply due to the transparent nature of the media under study. In fact, even transparent media can have a thermal effect which is far dominant to the effect of optical radiation pressure. For this reason, it is our intent to study and understand these effects as a necessary step in our work on optical radiation pressure.

When a beam of incident light passes through a medium, that medium may absorb some of the energy of the beam. This absorbed energy, in turn, will cause a change in temperature of the absorbing region of the media which then will diffuse to other parts of the medium and its surroundings in some regular way described by the thermal properties of the media involved. Because the index of refraction is a temperature dependant property, the temperature gradient also causes a

refractive index gradient. This causes a change in the optical path length in these regions to the partially absorbed beam of light as well as any other beam of light incident on the affected area of the media. This effect is referred to as thermal lensing and has been the focus of many other studies as an indicator of the optical and thermal properties of materials^{9,10}.

If a thermal lens is present during the course of an optical radiation pressure study, any far-field diffraction observed is actually the result of the superposition of the two lens effects. Our use of digital holography as an imaging method has proven to be a valuable indicator of both thermal and optical effects. With our continued work in thermal lensing, it is our goal to decouple these effects so that optical radiation pressure deformations may be easily observed. As will be discussed in detail below, these deformations will always result in a longer optical path length (positive phase shift) within the structure. Meanwhile, the thermal lensing effect results in a shortened optical path length (negative shift). Additionally, these two effects differ greatly in the time scale with which they occur. It is the subject of this and ongoing studies to make use of these differences to produce quantitative phase analyses of the two effects with excellent accuracy and precision.

2. THEORY

Both a 2D infinite and a 3D finite model have been developed to describe the thermal lens effect and the resulting phase shift for a cw laser induced mode-mismatched dual beam set up such as that used in the current study^{11,12}. The 2D infinite model has the assumption, among others, that the sample thickness is large enough that axial heat flow and sample edge effects can be ignored. This method becomes inadequate for the study of thin-film samples. The 3D finite model is able to successfully describe samples of all thicknesses; however, it lacks the convenient mathematical relation to thermo-optical properties like the 2D infinite model. Since these properties are typically not readily available for transparent media, the 2D infinite model is a preferred choice and it has proven adequate for our sample dimensions. It is the 2D infinite model that shall be described herein.

To maintain validity of the 2D infinite model, several assumptions are made and experimental design should take these into account. The sample cell thickness should be short compared to the confocal distance of the beams to ensure the spot size remains relatively constant through the sample. The sample cell dimensions should be large compared with the excitation beam radius so as both radial and axial edge effects can be ignored. The sample should absorb very little power to avoid convection effects. Finally, the temperature coefficient of refractive index, $\frac{dn}{dT}$, should be constant in the range of temperatures observed. With these assumptions in mind, the laser induced change in temperature within the sample can be described by¹¹,

$$\Delta T(r, t) = \frac{2P\alpha}{\pi C \rho w^2} \int_0^t \frac{1}{1 + 2t'/\tau} \exp\left(-\frac{2r^2/w^2}{1 + 2t'/\tau}\right) dt' \quad (1)$$

where r is the radial distance from the beam axis, t is the time of exposure to the excitation beam, P is the total excitation beam power at the sample, α , C , and ρ are the absorption coefficient, specific heat, and density of the sample, respectively, and w is the excitation beam radius in the sample. The characteristic thermal time constant, τ , is given by

$$\tau = \frac{w^2 C \rho}{4\kappa} \quad (2)$$

with thermal conductivity, κ . The resulting refractive index gradient can be described by,

$$n(r, t) = n_0 + \frac{dn}{dT} \Delta T(r, t) \quad (3)$$

where n_0 is the index of refraction at the starting temperature of the sample. This leads directly to phase shift described by,

$$\phi = \frac{2\pi}{\lambda} l [n(r,t) - n(0,t)] = \frac{2\pi}{\lambda} l \frac{dn}{dT} [\Delta T(r,t) - \Delta T(0,t)] \quad (4)$$

where λ is the wavelength of the probe beam and l is the thickness of the sample. Substituting Eq.(1) into Eq.(4), the phase shift can be rewritten as,

$$\phi = -\frac{P\alpha l (dn/dT)}{\kappa\lambda} \int_0^t \frac{1}{1+2t'/\tau} \left[1 - \exp\left(-\frac{2r^2/w^2}{1+2t'/\tau}\right) \right] \frac{dt'}{\tau} \quad (5)$$

This gives a complete time-resolved picture of the phase behavior due to the thermal effect. This is the model that has been tested in the current study to show that successful reduction of the thermal effect can be achieved by reduction of excitation time. In addition, Eq.(2) shows that the thermal time constant increases with the square of the excitation beam radius, thus making this an equally valuable parameter that can easily be controlled.

Now, the deformation effect of optical radiation is based on conservation of momentum across an interface as described by,

$$N \frac{n_1 h\nu}{c} \hat{z} = N \left(T \frac{n_2 h\nu}{c} - R \frac{n_2 h\nu}{c} \right) \hat{z} + \bar{p} \quad (6)$$

where n_1 and n_2 are the refractive index of the first and second media, respectively, N represents the number of photons, T and R are the transmission and reflection coefficients, and \bar{p} is the momentum transfer to the interface. By solving this equation for the simple case of a flat interface with normal incident photons,

$$\bar{p} = \frac{2n_1}{c} \left(\frac{n_1 - n_2}{n_1 + n_2} \right) N h\nu \hat{z} \quad (7)$$

it becomes easy to see that the direction of momentum transfer, and therefore the deformation of the interface, will always point in the direction of the smaller refractive index material regardless of the direction of beam propagation. This is because a photon gains momentum when moving into a higher refractive index medium. This phenomenon was shown by Ashkin and Dziedzic in 1973¹.

A relation between this exchange of momentum and the actual physical deformation must be derived. The forces that must be overcome in order to create a surface deformation are those associated with buoyancy and surface tension (or more appropriately, interfacial tension). Since our proposed deformations are of nanometric scale, it can be easily shown, for the media involved, that interfacial tension is by far the more dominant of the two. Thusly, buoyancy can be ignored in the present case. The force associated with interfacial tension has a direct mathematical relation to the contact angle of the deformation as follows,

$$\vec{F}_t = 2\pi w\sigma \sin \theta \hat{z} \quad (8)$$

with interfacial tension, σ , contact angle, θ , and w is the excitation beam radius as this is expected to be the radius of our induced deformation. This force must be balanced with the force associated with the incident excitation beam,

$$\vec{F}_{opt} = \frac{2n_1}{c} \left(\frac{n_1 - n_2}{n_1 + n_2} \right) P \hat{z} \quad (9)$$

where P is the excitation laser power just as above. Combining Eq.'s (8) and (9) and solving for θ we have,

$$\theta = \sin^{-1} \left(\frac{Pn_1(n_1 - n_2)}{c\pi w\sigma(n_1 + n_2)} \right). \quad (10)$$

Assuming a spherically growing deformation, we can use geometric relations to model the deformation height as a function of radial distance from the beam axis,

$$h(r) = h_0 + \frac{w}{\sin \theta} - \sqrt{\frac{w^2}{\sin^2 \theta} + r^2} \quad (11)$$

where h_0 is the maximum height of deformation (at $r=0$),

$$h_0 = \frac{w}{\sin \theta} \left(1 - \sqrt{1 - \sin^2 \theta} \right). \quad (12)$$

The phase shift then associated with this deformation would be,

$$\phi = h(n_1 - n_2) \frac{2\pi}{\lambda}. \quad (13)$$

With these approximations we have developed a computer simulation to combine thermal and optical models to better predict the experimental parameters necessary to decouple the two effects. Initial simulations show promising results for near term optical radiation pressure experiments. Figure 1 is an example simulation for benzyl alcohol and water, a promising pair of pure substances that will layer with a previously measured interfacial tension of 3.5mN/m^{15} . We begin by showing the predicted comparison of the two effects after a standard 2 second exposure to 700mW excitation from a $50\mu\text{m}$ radius beam (Figure 1A). Any optical pressure deformation at the interface would be completely masked by the thermal lens (TL). By reducing the exposure to only 10ms, we see the thermal effect is substantially reduced, however, any surface deformation is still expected to be below the detection limit and still strongly overwhelmed by the TL (Figure 1B). As mentioned above, increasing the excitation beam radius has a strong effect on the thermal time constant. Therefore, in Figure 1C we have increased the beam radius, but left the exposure time at 10ms to reduce the thermal effect while increasing the beam power to enhance the optical pressure effect. The combined model now predicts that

the optical pressure effect should dominate the phase image by more than .1 radian. This is well above the detection limit of our current setup and would be clearly evidenced in a successful conjugate experiment.

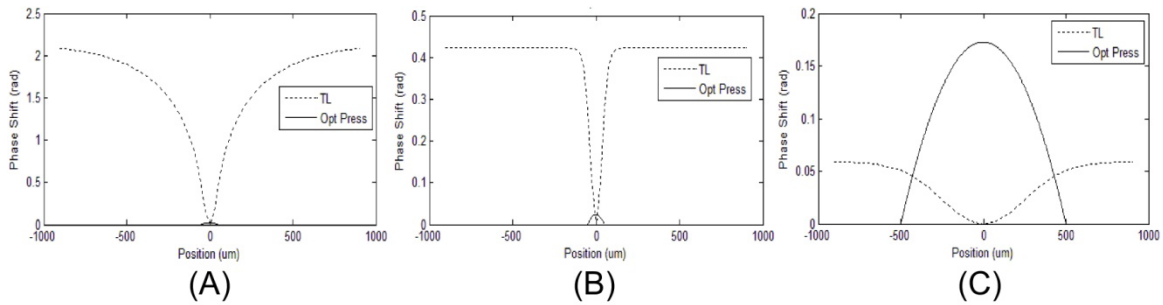


Figure 1. Model prediction for the thermal lens (TL) and optical pressure (Opt Press) effects for a sample of layered benzyl alcohol and water with an interfacial tension of 3.5mN/m. A) 700mW, 50 μ m beam excitation for a 2 second duration. B) Duration reduced to 10ms. C) 5W, 500 μ m beam excitation for 10ms.

3. METHODS

Figure 2 shows a diagram of the experimental apparatus. A Mach-Zehnder interferometer is used to create the hologram of the sample using low power (~ 2.5 mW) 633 laser light. The imaging beams (from a single source) are delivered by a 50:50 split fiber optic cable (reference/probe beams), which are then collimated and passed through polarizers upon entering the system. The polarizers can be adjusted to aid in beam level balancing. The two beams then pass through matched microscope objectives before being superposed by the beam combiner, differing only in that the probe beam path includes the transparent sample area as shown. The resulting hologram is recorded by a digital CCD camera placed atop the setup and passed into our LabVIEW personal computer platform for amplitude and phase reconstruction based on the angular spectrum method¹³.

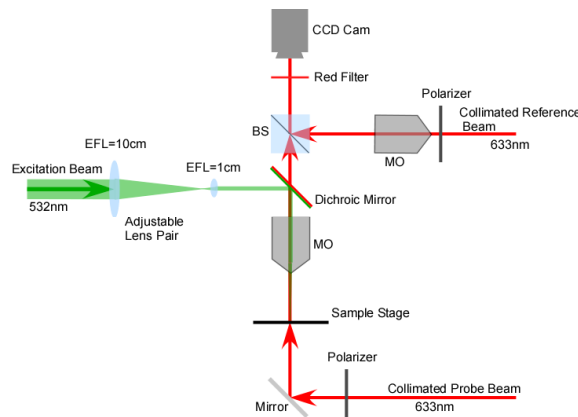


Figure 2: Experimental apparatus (color online). The excitation beam (green) is focused downward through the sample by the probe-shared microscope objective (MO). The probe beam (red) is the object arm of the Mach-Zehnder interferometer and passes upward through the sample, combines with the reference beam, and creates the hologram captured by the CCD camera.

An integrated optical excitation arm delivers a high powered 532 cw laser beam to the system via a fiber optic cable and collimation setup. The beam is then passed through a 10:1 focal length lens pair to create a much reduced collimated beam radius. A dichroic mirror reflects this excitation beam down toward the sample while allowing the probe beam to transmit up toward the CCD camera. The excitation beam passes through the shared microscope objective which condenses the already thin beam through the sample area. The microscope objectives are chosen to have long effective focal lengths to aid in meeting the requirements of the 2D infinite model described above. A removable red filter is placed just in front of the CCD camera to filter any 532 excitation light leaking through the dichroic mirror. This “leaky” light, however, can be used to find the excitation beam radius and spot location as well as its waist along the beam axis by temporarily removing the red filter. The excitation beam radius, w , is defined as the radius at which our Gaussian

beam amplitude reduces to e^{-2} of its maximum value. With the red filter in place, a hologram, containing complete phase and amplitude information, is captured by the CCD camera and processed by our software routines to reconstruct the phase image in real time both with and without excitation.

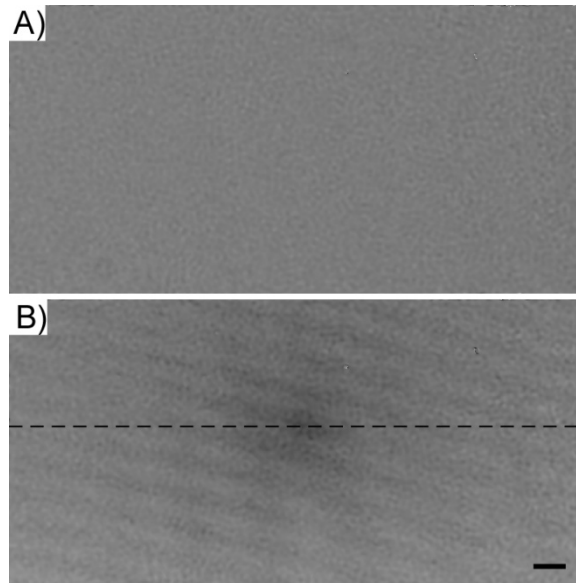


Figure 3: Phase images of a sample, A) with no excitation and B) with optical excitation. The phase scale of both images ranges from 0 (black) to 2π (white) and the spatial scale bar is $100\mu\text{m}$. The dashed line indicates the selected cross-section used for further analysis.

The sample consists of pure methanol in a standard glass cuvette of cross-sectional area, 5mm by 10mm, with a sealable lid. This sample is placed on the sample stage on its side oriented with a 5mm path length. While viewing the phase image, with the optical excitation beam at 750mW (at the sample), the object stage was translated along the beam path (z direction) until the focus of the excitation beam was centered within the sample. At this position, a well defined phase signal, i.e. the thermal lens, was clearly observed (Figure 3). A cross-section through the center of this image was used to plot the profile of the phase shift as a function of radial distance from the z-axis of the excitation beam (Figure 4). It should be noted that, due to the time-sensitivity of the thermal effect, attention must be given to excitation beam exposure time to ensure measurements are taken in the proper regime. All measurements for the purpose of determination of absorption coefficient, for example, were performed at exposure times greater than 2000τ to ensure steady-state regime was reached. Though the model is time-resolved, steady-state measurements eliminate time factors as a source of possible error while determining the absorption coefficient. With the absorption coefficient successfully determined, the time-resolution of the model was tested by recording images at high speed to capture the entire excitation event at various short time intervals.

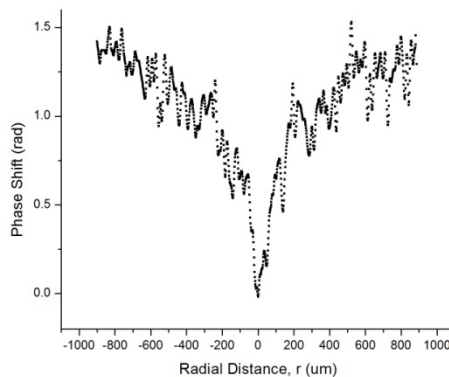


Figure 4: Cross-sectional profile of the thermal lens shown in Figure 3B (dashed line).

4. RESULTS

The absorption coefficient of methanol was determined in a previous experiment similar to that described above¹⁴. This value and the other experimental parameters for methanol are listed in table 1. The data from several times during the excitation event are displayed in figure 4 as scatter plots with the model predictions superposed as solid line plots. There is clearly excellent agreement between the predicted and experimental values.

Table 1: Experimental parameters for methanol.

w	50 μm
l	5mm
dn/dT	$-3.9 \times 10^{-4} \text{ } ^\circ\text{C}^{-1}$
κ	.202W/m $^\circ\text{C}$
λ	633nm
P	750mW
τ	4.7ms
t	0 – 1500ms
α_{exp}	$3.6 \times 10^{-4} \text{ cm}^{-1}$

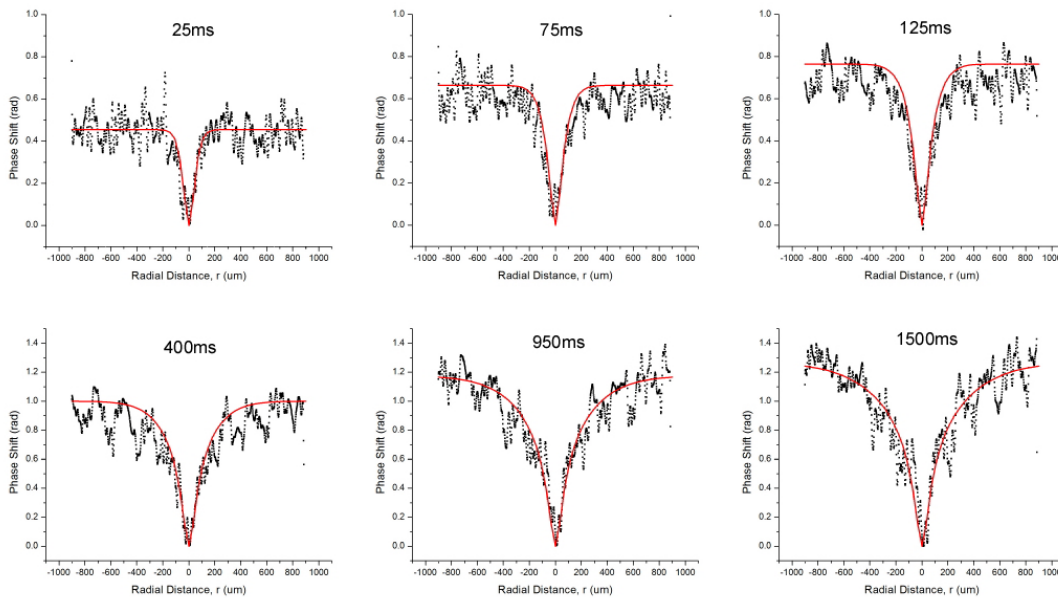


Figure 5. Experimental data (scatter plots) and 2D infinite model predictions (solid lines) at several time-resolved stages of the thermal lens excitation event.

5. DISCUSSION

The time resolution study shows excellent agreement with the predictions of the 2D infinite model. This is an important step towards imaging the small optical radiation pressure deformations that would typically be dominated by the thermal lens. As mentioned earlier, reducing the thermal effect can not only be achieved by reducing the time scale of observation, but also by increasing the excitation beam radius. Since the thermal time constant will increase with the square of the beam radius, this is arguably a more important parameter than further reducing the time scale of the excitation. The effect on the total height of deformation is only minimally affected by this adjustment.

We are currently working with benzyl alcohol, which has a measured interfacial tension with water of only 3.5 mN/m¹⁵. Initial simulations, shown above, suggest that, using our current method, we will be able to successfully observe and

measure the deformation of this interface on the order of 10's of nanometers. The current setup is under adjustment to allow for the predicted necessary parameters, however, we have performed preliminary measurements to test the behavior of benzyl alcohol. Figure 6 shows the comparison of these measurements with those predicted by our model with excellent agreement. Once we have characterized our method with such known materials, we aim to determine unknown interfacial tensions by measuring these deformations with high precision.

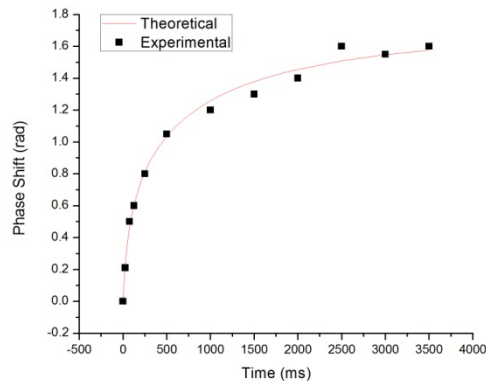


Figure 6. Time-resolved thermal lens phase shift measurements (at $r=900\mu\text{m}$) of benzyl alcohol with model prediction (solid line).

With continued success in measuring optical radiation pressure deformations and determining interfacial tensions, we will be very interested in using the technique to study biological cell membranes. The membrane-fluid interface should be very similar to the fluid-fluid interface currently under investigation. It is expected that our high precision technique can be adapted to the characterization of physical properties of cellular membranes and structures.

Noise levels of our system were measurement by imaging the sample with no excitation beam present and taking the standard deviation of this phase profile to indicate background noise. Values ranged between .03 and .09 radians during the course of these experiments. The optical path length change, therefore, has been measured to better than 9nm resolution. This is equivalent to a 40nm deformation for the upcoming study of benzyl alcohol and water. It is expected that, with careful isolation and construction, future apparatus could improve this precision by up to an order of magnitude.

6. CONCLUSION

We continue to make strides in imaging optical and thermal phenomenon with high precision by digital holography. We have implemented a method of reducing our excitation exposure time into the time resolved regime of the 2D infinite model for thermal lensing. This was done both to test the completeness of the model as well as to reduce the thermal effect on the media to a level that other optical phenomenon may be observed without the dominating effect of thermal lensing present. The near perfect match between the time-resolved model and our phase measurement is very promising for our near and long term interests. Of particular near-term interest to us is the nanometric measurement of optical pressure deformation from photon momentum exchange across a fluid interface. The results of this study and our computer simulations suggest that decoupling the two effects and imaging with digital holography should prove successful for fluid-fluid interfaces.

This work is supported in part by the National Science Foundation, grant number 0755705.

REFERENCES

- [1] Ashkin, A. and Dziedzic, J.M., "Radiation Pressure on a Free Liquid Surface," *Phys. Rev. Lett.* 30, 139-142 (1973).
- [2] Casner, A. and Delville, J.-P., "Adaptive Lensing Driven by the Radiation Pressure of a Continuous-Wave Laser Wave Upon a Near-Critical Liquid-Liquid Interface," *Opt. Lett.* 26(18), 1418-1420 (2001).

- [3] Chraïbi, H., Lasseux, D., Arquis, E., Wunenburger, R., Delville, J.-P., "Simulation of an Optically Induced Asymmetric Deformation of a Liquid-Liquid Interface," *Eur. J. Mech. B/Fluids*, 27, 419-432 (2008).
- [4] Sakai, K., Mizuno, D., and Takagi, K., "Measurement of Liquid Surface Properties by Laser-Induced Surface Deformation Spectroscopy," *Phys. Rev. E*, 63, 046302 (2001).
- [5] Cuche, E., Bevilacqua, F., Depeursinge, C., "Digital holography for quantitative phase-contrast imaging," *Opt. Lett.*, 24(5), 291 (1999).
- [6] Mann, C. J., Yu, L., Lo, C.-M., and Kim, M. K., "High-resolution quantitative phase-contrast microscopy by digital holography," *Opt. Express*, 13, 8693 (2005).
- [7] Mitani, S., Sakai, K., "Measurement of ultralow interfacial tension with a laser interface manipulation technique," *Phys. Rev. E*, 66, 031604 (2002).
- [8] Yoshitake, Y., Mitani, S., Sakai, K., Takagi, K., "Measurement of high viscosity with laser induced surface deformation technique," *J. Appl. Phys.*, 97, 024901 (2005).
- [9] Marcano, A., Loper, C., Melikechi, N., "High sensitivity absorption measurement in water and glass samples using a mode-mismatched pump-probe lens method," *Appl. Phys. Lett.*, 78, 3415-3417 (2001).
- [10] Cabrera, H., Marcano, A., and Castellanos, Y., "Absorption coefficient of nearly transparent liquids measured using thermal lens spectrometry," *Condensed Matter Physics*, 9, No. 2(46), 385-389 (2006).
- [11] Shen, J., Lowe, R. D., and Snook, R. D., "A model for cw laser induced mode-mismatched dual-beam thermal lens spectrometry," *Chem. Phys.*, 165, 385 (1992).
- [12] Shen, J., Baesso, M. L., and Snook, R. D., "Three-dimensional model for cw laser-induced mode-mismatched dual-beam thermal lens spectrometry and time-resolved measurements of thin-film samples," *J. Appl. Phys.*, 75, 3738 (1994).
- [13] Yu, L. and Kim, M. K., "Wavelength-scanning digital interference holography for tomographic 3D imaging using the angular spectrum method," *Opt. Lett.* 30, 2092 (2005).
- [14] Clark, D. C. and Kim, M. K., "Determination of absorption coefficient by digital holographic measurement of optical excitation," *App. Opt.*, (submitted) (2010).
- [15] Kim, H. and Burgess, D. J., "Prediction of interfacial tension between oil mixtures and water," *J. Colloid Interface Sci.*, 241, 509-513 (2001).